Isotope effects in the electronic spectrum of S^+ and Se^+ in silicon

B. Pajot
GPS, UMR 75-88 du CNRS, Universités Pierre et Marie Curie et Denis Diderot, Campus Boucicaut, 140 rue de Lourmel, 75015 Paris, France

B. Clerjaud
LOS, UMR 76-01 du CNRS, Université Pierre et Marie Curie, 140 rue de Lourmel, 75015 Paris, France

M. D. McCluskey
Washington State University and Institute for Shock Physics, Pullman, Washington 99134-2814, USA
(Received 14 October 2003; published 27 February 2004)

Weak satellites of the strong and sharp parity-forbidden, but symmetry-allowed $1s(A_1) \rightarrow 1s(T_2)$ doublet of the S^+ donor spectrum in silicon are reported. The low-energy ones are ascribed to a Si isotope effect and the high-energy ones to an S isotope effect. We also show that the profile of the low-energy component of the same transition of Se^+ in silicon can be reproduced from the computed combination of Si and Se isotope shifts with the same characteristics as those of S^+, but with a smaller Se isotope shift. The Si isotope shift is discussed in terms of the bond softening effect in the electronic ground state for a cluster involving the chalcogen atom and its first nearest neighbors. The positive chalcogen isotope shift is discussed by considering the effect of a vibronic coupling to the τ_2 mode of vibration in the excited state within the bond softening framework. It is also shown that this vibronic coupling can account for the noneffective mass behavior of the $1s(T_2)$ level.

DOI: 10.1103/PhysRevB.69.085210 PACS number(s): 78.30.Am, 71.55.Cn

I. INTRODUCTION

Isotope shifts (ISs) of vibrational lines are commonly observed by infrared (IR) absorption or Raman scattering when more than one isotope of the atom involved in the vibration is present and when the lines are reasonably sharp. The lines are always shifted to lower energies when the atom is replaced by a heavier isotope as the vibrational energy is inversely correlated to the mass of the atom. In solid state spectroscopy, this negative IS is used to identify or check the nature and number of isotopic species present in defects or impurity complexes. ISs of electronic lines are less common and they are usually seen in high-energy photoluminescence or absorption lines and they are related with the coupling of the electronic levels to local vibrational modes. At a difference with the vibrational ISs, the electronic ISs can be positive or negative with respect to the lighter isotope and the prediction of these shifts requires a detailed analysis of the coupling between the electronic and vibrational states. Such shifts have been reported for instance for C complexes produced in silicon by electron irradiation,[1] but also in the spectra of different substitutional transition metals in compound semiconductors.[2,3]

In silicon, substitutional chalcogen atoms (S, Se, and Te) have two more valence electrons than Si. The binding energy of the first electron is rather large ($\sim$0.3 eV for S and Se) compared to that for group V donors P and As in silicon ($\sim$0.05 eV), but within shifts of their positions, the electronic line spectra of S^0, Se^0, P, and As donors are strikingly similar as they involve effective-mass-like excited states. The $1s$ state displays the sixfold degeneracy of the conduction band of silicon, but this degeneracy is lifted by the central cell effect and the $1s(A_1)$ state can be substantially deeper than the $1s(E)$ and $1s(T_2)$ states[4,5] (A_1, E, and T_2 are irreducible representations of the tetrahedral point group T_d). In silicon, the Raman scattering of the $1s(A_1) \rightarrow 1s(E)$ transition for P and As (Refs. 6 and 7) as well as the IR absorption of the symmetry-allowed $1s(A_1) \rightarrow 1s(T_2)$ doublet of Bi (Ref. 8) have been observed. The doublet structure of the $1s(A_1) \rightarrow 1s(T_2)$ transition is due to a spin-valley coupling made possible by the p-like character of the T_2 levels.

The ground state of the second electron of S and Se is near 0.6 eV, in the middle of the silicon energy gap. The line spectra of S^+ and Se^+ bear similarities with those of S^0 and Se^0, but the spacings between corresponding lines are four times larger than for the neutral charge state.[9] The factor of 4 comes from the quadratic dependence of these energies on the $+2q$ charge of the nucleus. The singly ionized charge state is paramagnetic and the electron paramagnetic resonance (EPR) of S^+ in silicon shows that this ion has a cubic symmetry in the silicon lattice.[10] The absorption spectra of the chalcogen atoms and of their complexes, like the chalcogen pairs, have been extensively investigated in silicon,[9] and the ground state energies are the greatest for the isolated atoms. In silicon, when chalcogens are partially compensated, for instance with acceptors, it is possible to observe the spectra of the singly ionized donors. In addition to the usual effective-mass-like lines, the ionized chalcogen spectra show rather intense parity-forbidden $1s(A_1) \rightarrow 1s(T_2)$ transitions and weaker $1s(A_1) \rightarrow ns(T_2)$ transitions.

With the exception of the H/D isotope effect involving tunneling hydrogen of a donor complex in germanium,[11] no clear evidence of an isotope effect has been reported so far in the absorption spectra of effective-mass-like donor and acceptors in semiconductors. We present here results showing two distinct isotope effects of some electronic transitions of the S^+ donor ion in silicon. We discuss them in terms of the

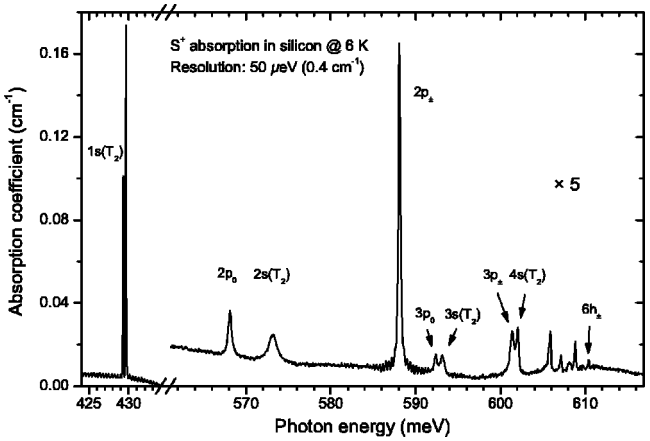

FIG. 1. Medium resolution overall spectrum of singly ionized sulfur in silicon (sample 1). The abscissa scale is the same for both sections. The ordinates of the right-hand side section have been expanded by a factor of 5.

coupling of this ion with the neighboring atoms and we extrapolate the results to the Se^+ ion.

II. EXPERIMENTAL SETUP AND RESULTS

The spectra were obtained at 6 K with a BOMEM DA8 Fourier transform spectrometer. An optical filter with a high-frequency cutoff at 0.7 eV was placed between the quartz-halogen source and the samples to prevent the trapping of electrons from the photogenerated electron-hole pairs by the positive chalcogen ions. The S^+ spectrum was measured in a float-zone boron-doped silicon sample (sample 1). This sample had been diffused with ^{17}O and ^{18}O for a long time at high temperature in a cell used previously for S diffusion. The S pollution was detected by the unexpected observation in one chip of this sample, of lines of the S^+ spectrum, and this allowed the measurements discussed here. Sample 2, doped with sulfur enriched with about 25% ^{33}S, was measured in a multitreflection geometry[12] allowing an effective sample thickness of 15 mm. Silicon samples containing Se^+ and Te^+ with natural isotopic abundances were also measured during this study.

A. The S^+ spectrum

The spectrum of S^+ in sample 1 is shown in Fig. 1. In this figure, the most prominent lines are labeled according to the final states of the transitions, following the notations of Kohn and Luttinger.[4] The two strong lines near 429 meV originate from the $1s(A_1) \rightarrow 1s(T_2)$ transition split by some modified spin-orbit (spin-valley) splitting of the $1s(T_2)$ level. The line with the lowest energy corresponds to the doubly degenerate Γ_7 spin representation of T_d and the one with the highest energy to the fourfold degenerate Γ_8 representation.[5] Doublets are observed near the transitions expected toward the $3p_0$ and $3p_\pm$ states. From energy considerations, the low-energy components are ascribed to the $3p_0$ and $3p_\pm$ lines and the high-energy ones to the $3s(T_2)$ and $4s(T_2)$ lines, respectively. The highest energy line of this spectrum is attributed to $6h_\pm$ (see Table I). All the S^+ lines observed in sample 1 are reported in Table I. The line reported at 598.52 meV by Krag *et al.* and attributed to $3d_0$ (Ref. 13) is not observed here, but the observation of five lines above $3p_\pm$, the highest energy line of the S^+ spectrum reported so far,[13] means that the sample is of a high quality for the present purpose. The single donor effective-mass (EM) energies of Table I are those calculated in Ref. 14.

TABLE I. Positions and full widths at half-maximum (FWHM) at 6 K of the S^+ lines measured in sample 1 (all quantities are expressed in meV). The energies of the excited levels (fourth column from the right) are normalized by taking for the $3p_\pm$ state an energy four times the value calculated in the effective mass (EM) approximation (second column from the right). The corresponding ground state energy (613.8 meV) is slightly larger than the ones quoted in the literature [613.5 and 613.6 meV (Refs. 5 and 13)]. The $2p_\pm$ line, reported as a doublet[15] shows a high-energy asymmetry, but the position given here is the measured peak value.

Line label	Position	Energy	Energy/4	Calculated (EM)	FWHM
$1s(T_2)\Gamma_7$	429.23	184.57	46.14	31.26	0.022
$1s(T_2)\Gamma_8$	429.60	184.20	46.05		0.030
$2p_0$	568.03	45.77	11.44	11.49	0.5
$2s(T_2)$	573.14	40.66	10.17	8.86	1.1
$2p_\pm$	588.01	25.79	6.45	6.40	0.25
$3p_0$	592.27	21.53	5.38	5.48	0.3
$3s(T_2)$	593.04	20.76	5.19	4.78	0.4
$3p_\pm$	601.32	[12.48]	[3.12]	**3.12**	0.4
$4s(T_2)$	601.99	11.81	2.95	2.91	0.3
$4p_\pm$ and $5s(T_2)$	605.80	8.00	2.00	2.19 and 1.93	0.3
$5f_0$	607.05	6.75	1.69	1.63	0.2
$5p_\pm$	608.07	5.73	1.43	1.45	0.4
$5f_\pm$	608.76	5.04	1.26	1.26	0.2
$6h_\pm$	610.32	3.48	0.87	0.89	0.2

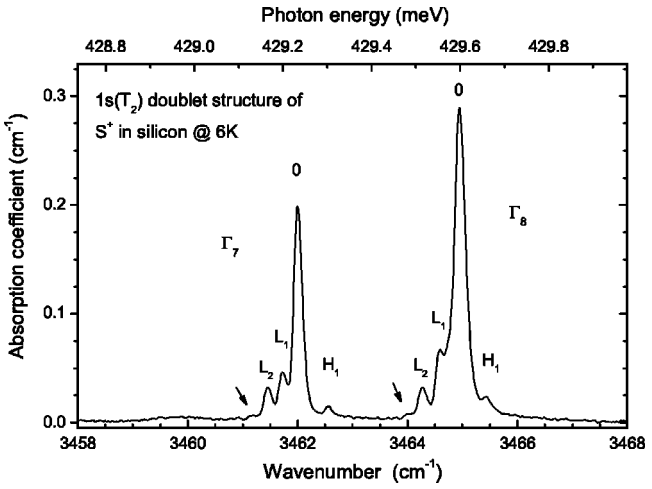

FIG. 2. Fine structure of the $\Gamma_7-\Gamma_8$ doublet of $1s(T_2)$ of S^+ in sample 1. The L_i and H_1 satellites are isotopic components. The full widths at half-maximum of $0(\Gamma_7)$ and $0(\Gamma_7)$ are 22 and 30 μeV, respectively, and their separation is 0.365(4) meV. The features attributed to $^{28}Si_2^{29}Si^{30}Si$ are indicated by arrows. The resolution is 3.7 μeV (0.03 cm^{-1}).

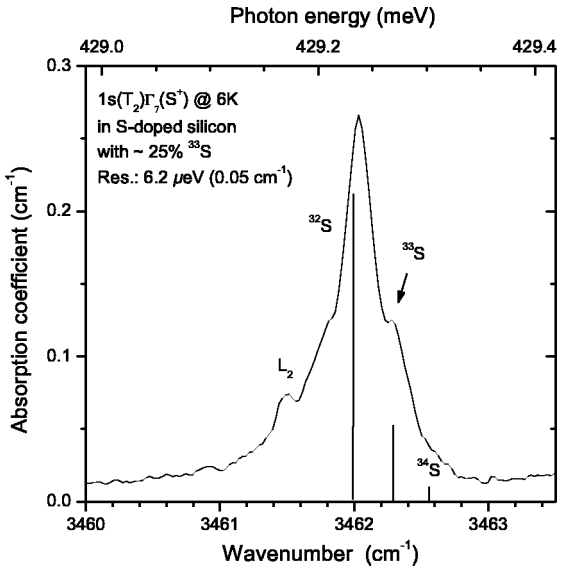

FIG. 3. $1s(T_2)\Gamma_7$ of S^+ in sample 2. The heights of the bars indicating the positions of the ^{32}S, ^{33}S, and ^{34}S components are proportional to the abundances of the isotopes. The positions of the ^{32}S and ^{34}S components are taken from the data with sample 1 and the attribution of L_2 is given in Table II.

The detection of the S^+ spectrum is due to the presence of boron in the sample. The B^- ions can scatter the electrons still bound to S ions, especially in highly excited states. A consequence would be a broadening of the levels (Stark broadening), but the sharp lines near the continuum show that this mechanism is not dominant in this sample. The relatively large full width at half-maximum (FWHM) of $2s(T_2)$ can be due to the unresolved splitting between the Γ_7 and Γ_8 states.

B. The $1s(T_2)$ components of S^+

Uniaxial stress studies have shown that the $1s(T_2)$ states cannot be described by the deformation potential approximation and that they are less sensitive to stress than the effective mass states, including the other $ns(T_2)$ states.[16] This is also seen in the FWHMs of the $1s(T_2)\Gamma_7$ and $1s(T_2)\Gamma_8$, labeled from now Γ_7 and Γ_8, which are about one order of magnitude smaller than those of the other lines of the spectrum (see Table I). A close-up of these two lines is shown in Fig. 2. They both present unexpected low-frequency satellites and a weak high-frequency one. The low-energy satellites are reminiscent of those due to Si isotope effects in vibrational spectra like those of interstitial oxygen.[17] The high-frequency satellite can be related to the ^{34}S isotope, whose natural relative abundance with respect to ^{32}S is 0.045. No contribution of ^{33}S, expected to lie midway between the ^{32}S and ^{34}S components, is detected in this sample. This can be understood as $[^{33}S]/[^{32}S]$ in natural sulfur is only 0.008 and the ^{33}S component would be located on the low energy onset of the strong ^{32}S line (to be exhaustive, $[^{36}S]/[^{32}S]$ is 2.1×10^{-4}).

The same Γ_7 structure as in Fig. 2 is shown in Fig. 3 for sample 2, enriched with about 25% of isotope ^{33}S. In this latter structure, a high-energy component is now clearly visible at the position expected for ^{33}S. This result confirms the existence of a positive S isotope shift of the Γ_7 line. As the individual FWHMs are larger for Γ_8 (see Table I), the isotope effect is less distinct for that line in sample 2 and it is not shown here, but the positive isotope shift of S for Γ_8 must be considered as established. The ISs observed in sample 1 are level-dependent (see Table II). We can substantiate the Si isotope guess by considering a SSi_4 quasimolecule or cluster interacting weakly with the crystal. From the natural abundances of ^{28}Si, ^{29}Si, and ^{30}Si (0.922, 0.047, and 0.031, respectively), the four most probable surroundings of a S atom are $^{28}Si_4$, $^{28}Si_3^{29}Si$, $^{28}Si_3^{30}Si$, and $^{28}Si_2^{29}Si^{30}Si$. The ratios of the probabilities of the $^{28}Si_3^{29}Si$, $^{28}Si_3^{30}Si$, and $^{28}Si_2^{29}Si^{30}Si$ surrounding combinations normalized to $^{28}Si_4$ are thus 0.20, 0.13, and 0.02, respectively. The first two values compare with the measured values of 0.21 and 0.15 for the intensities ratios $L_1(\Gamma_7)/0(\Gamma_7)$ and $L_2(\Gamma_7)/0(\Gamma_7)$. The

TABLE II. Shifts (μeV) from the 0 lines of the $1s(T_2)$ isotope satellites of S^+ (accuracy, ±7 μeV). The positions of the $0(\Gamma_7)$ and $0(\Gamma_8)$ lines are 429.233 and 429 599 meV, respectively (accuracy, ±3 μeV). The same value of 35 μeV is obtained for the ^{33}S shift of the Γ_7 line either by linear interpolation with the ^{34}S value (sample 1) or by direct measurement (sample 2). The last line is an estimation of the shifts of the components noted by arrows in Fig. 2.

Satellite	$1s(T_2)\Gamma_7$	$1s(T_2)\Gamma_8$	Attribution
H_1	+69	+59	$^{34}S^{28}Si_4$
	+35		$^{33}S^{28}Si_4$
0	-	-	$^{32}S^{28}Si_4$
L_1	−34	−44	$^{32}S^{28}Si_3^{29}Si$
L_2	−69	−84	$^{32}S^{28}Si_3^{30}Si$
	−100	−120	$^{32}S^{28}Si_2^{29}Si^{30}Si$

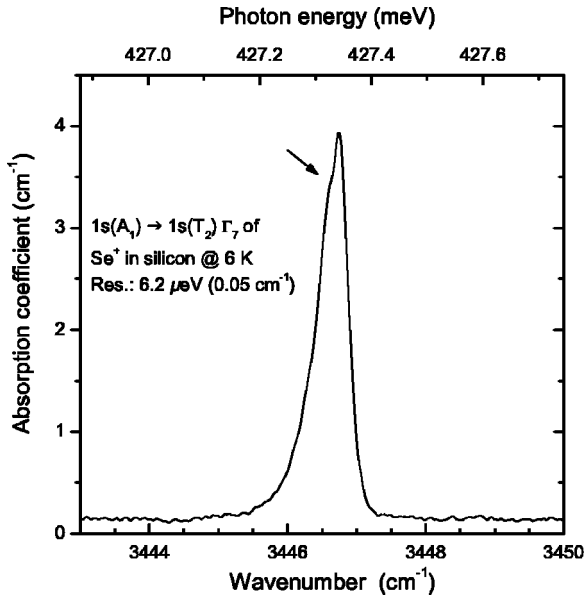

FIG. 4. $1s(T_2)\Gamma_7$ components of Se^+ in silicon with the same abscissa scale as Fig. 2. The separation from $1s(T_2)\Gamma_8$ (not shown) is 2.27 meV.

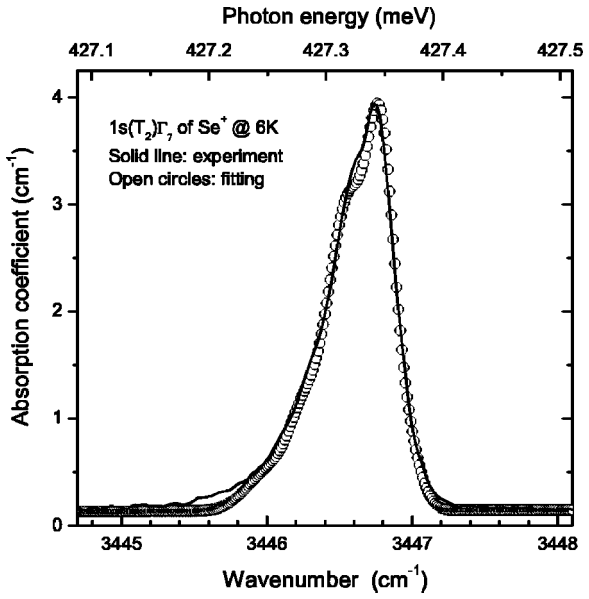

FIG. 5. Peak fitting of $1s(T_2)\Gamma_7(Se^+)$ profile of Fig. 4 with Si and Se isotope effects. It is obtained by summing the intensities of 18 individual Gaussian components with the same FWHM of 27 μeV, knowing the isotope relative abundances and fitting the peak absorption of $^{80}Se^{28}Si_4$ to 3.28 cm^{-1}. The energy scaling is obtained from the Se and Si ISs (+11 and −34 μeV/nucleon, respectively), combined with the fitted energy of the $^{80}Se^{28}Si_4$ component (427.346 meV).

very weak features noted by arrows in Fig. 2 are attributed to the $^{28}Si_2^{29}Si^{30}Si$ surrounding. The relative intensities of the Si combinations scale with the fourth power of the Si isotopic abundances and this is also consistent with the existence of four equivalent Si atoms surrounding the S atom. The relative intensity of $H_1(\Gamma_7)$ with respect to $0(\Gamma_7)$ is ~0.05 and it compares well with the relative abundance of ^{34}S, so that the attribution of 0 and H_1 to the zero-phonon lines of ^{32}S and ^{34}S seems to be sensible. Moreover, as seen above, this is substantiated with the observation of the ^{33}S IS in sample 2. The observation of ISs associated with the $2p_\pm$ line would have been instructive, but that line is unfortunately too broad (see Table I).

C. The $1s(T_2)\Gamma_7$ component of Se^+

The ionization energy of Se^+ in silicon (593 meV) is only slightly lower than that of S^+ and we have looked for similar isotope effects for the $1s(T_2)$ line of Se^+ in silicon. The profile of $1s(T_2)\Gamma_7$ of Se^+ is shown at 6 K in Fig. 4 with the same abscissa scale as that of Fig. 2 [$\Gamma_8(Se^+)$ is outside the span of the figure]. The low-energy side of $\Gamma_7(Se^+)$ is about two times broader than the high-energy side and no structure is observed but a shoulder, noted by an arrow in Fig. 3. The Se isotopes are ^{74}Se, ^{76}Se, ^{77}Se, ^{78}Se, ^{80}Se, and ^{82}Se with natural abundances of 0.009, 0.094, 0.076, 0.238, 0.496, and 0.087, respectively. For the fitting procedure, the shifts are assumed to have the same signs as for S^+ and they are adjusted to fit the experimental profile. Besides the most intense components, the contributions of $^{74}Se^{28}Si_4$, $^{78}Se^{28}Si_2^{29}Si^{30}Si$, and $^{80}Se^{28}Si_2^{29}Si^{30}Si$ have also been included. The best fit is shown in Fig. 5. Despite small differences due to the crudeness of the assumptions used, specially concerning fully symmetric Gaussian components, the overall agreement with the observed profile seems to be a proof of the role of isotope effects in the $\Gamma_7(Se^+)$ line shape. This fit is obtained with a FWHM of 27 μeV, a Se IS of only +11 μeV/nucleon, anticipated from the heavier mass of the Se atom compared to sulfur, and a Si IS of −34 μeV/nucleon, close to the one for sulfur. The fit shows also that the individual components of $\Gamma_7(Se^+)$ stay sharp. Component $\Gamma_8(Se^+)$ has an observed FWHM near 250 μeV and it does not show the assymmetry of $\Gamma_7(Se^+)$ so that no isotope fitting has been tried on that component. The ionization energy of Te^+ in silicon is 411 meV and the $1s(T_2)\Gamma_7$ component has a FWHM of 223 μeV, with a very slight low-energy broadening. Considering the S and Se ISs values, a Te IS of +5 μeV/nucleon seems to be a reasonable estimation. Leaving the Si IS unchanged, we expect from the Te isotopes distribution an upper limit of the FWHM of $\Gamma_7(Te^+)$ comparable to that of $\Gamma_7(Se^+)$. The fact that the former is more than three times larger than the latter means that $\Gamma_7(Te^+)$ is broadened by mechanisms other than isotope effect. The ISs measured or adjusted for S and Se are given in Table III.

TABLE III. Isotope shifts per nucleon (μeV) measured for the S^+ lines and obtained from the fit for the Se^+ line.

Impurity	Sulfur		Selenium
Transition	$1s(T_2)\Gamma_7$	$1s(T_2)\Gamma_8$	$1s(T_2)\Gamma_7$
Chalcogen shift	+34±3	+30±5	+11
Silicon shift	−34±3	−43±5	−34

III. DISCUSSION

A. The Si isotope shift

Two distinct ISs are reported here: one, positive, related to the chalcogen atom and a second one, negative, related to the surrounding Si atoms. It must be noted that opposite ISs due to C and Si have already been reported for carbon-related complexes produced in silicon by electron irradiation.[1] We discuss the ISs reported here in the frame of a tetrahedral XSi_4 cluster (X is S or Se) in the valence force approximation. In II–VI compounds, the radial force constant is much larger than the transverse one[18] and to simplify, we assume that this also holds for silicon so that we neglect the latter. Within this approximation, there are only two vibrational modes of the cluster: a fully symmetric one, α_1, and a triply degenerate asymmetric one, τ_2, transforming, respectively, according to the Γ_1 and Γ_5 irreducible representations of the T_d point group.

Let us consider first the vibronic coupling with the α_1 mode. In this case, the energy E of an optical transition has three contributions: (i) a purely electronic one, (ii) one involving lattice relaxation, and (iii) one coming from the zero-point energies in the electronic ground and excited states. To the first order, the force constants do not depend on the atom masses and therefore, the lattice relaxation energies do not show any isotope effect. For the above-considered XSi_4 cluster, the zero-point energy contribution to E due to the α_1 and τ_2 modes is

$$\frac{\hbar}{2}[(\omega_1^e-\omega_1^g)+3(\omega_5^e-\omega_5^g)], \tag{1}$$

where the index j of the mode frequency ω refers to one of the irreducible representations Γ_j of T_d and the superscript to the excited (e) or ground (g) state. When one of the Si atoms of the cluster is replaced by an isotope Si^i, the point group symmetry of the XSi_3Si^i cluster changes to C_{3v}. The τ_2 mode with frequency ω_5 splits then into two modes with frequencies ω_{51} and ω_{53}, transforming as the singly degenerate Γ_1 and doubly degenerate Γ_3 representations of the C_{3v} group, respectively, while the frequency of the singly degenerate α_1 modes shifts from ω_1 to ω_{11}. The zero-point energy contribution to the energy E_i of the optical transition for the XSi_3Si^i cluster becomes

$$\frac{\hbar}{2}[(\omega_{11}^e-\omega_{11}^g)+(\omega_{51}^e-\omega_{51}^g)+2(\omega_{53}^e-\omega_{53}^e)] \tag{2}$$

and the electronic Si IS δ_{Si} is the difference between expressions (2) and (1). If the frequencies of the modes are the same in the electronic ground and excited states, δ_{Si} is zero. One condition put forward to explain the observation of an IS is a difference of the electronic densities at the atom site in the ground and excited states:[19] an excess electron localized in the vicinity of the cluster softens the force constants between the atoms of the cluster as it corresponds to a filling of antibonding orbitals associated with the bonds. This results in a reduction of the frequencies of the modes of the cluster in the ground state, compared to the excited state where the electronic density is smaller. Expressions for the above frequencies can be derived from the work of Rosenthal.[20] Within the valence force approximation, $\omega_{11}=\omega_1\sqrt{1-\kappa}$, $\omega_5=\omega_{53}=\omega_1\sqrt{1+\Lambda}$, and $\omega_{51}=\omega_1\sqrt{1+\Lambda-3\kappa}$, where $\omega_1=\sqrt{k/m}$ is the frequency of the α_1 mode. The quantities $\kappa=\Delta m/4(m+\Delta m)$ and $\Lambda=4m/3M$ are expressed in terms of the mass M of atom X and of the masses m and $m+\Delta m$ of the ^{28}Si and ^{i}Si atoms. The IS δ_{Si} thus reads

$$\delta_{Si}=\frac{\hbar}{2}[(\omega_{11}^e-\omega_1^e)-(\omega_{11}^g-\omega_1^g)+(\omega_{51}^e-\omega_5^e)-(\omega_{51}^g-\omega_5^g)]. \tag{3}$$

When an electron is bound to a donor, the more localized the electron, the weaker the force constant: the X–Si spring constant k is smaller in the ground state (k_g) than in the excited state (k_e). For $\kappa \ll 1$, the explicit form for δ_{Si} is

$$\delta_{Si}=\frac{-\hbar\omega_1^e}{4}\kappa\left[1+\frac{3}{\sqrt{1+\Lambda}}\right]\left(1-\sqrt{\frac{k_g}{k_e}}\right). \tag{4}$$

With the above assumption, the value of expression (4) is negative, as observed. In order to evaluate the bond softening, an estimation of ω_1^e is required. A resonance ascribed to P^+ has been reported[21] in silicon at 55 meV ($\approx$445 cm^{-1}). Besides the nuclear charge, the mass and electronic structure of S^+ are close to those of P^+ so that a mode frequency of 500 cm^{-1} is of the right order of magnitude for S^+. In order to match the experimental values of the $^{32}S^{28}Si_4$–$^{32}S^{28}Si_3^{29}Si$ IS (-34 μeV) for the transition towards the $1s(T_2)\Gamma_7$ level of S^+, the ratio k_g/k_e deduced from expression (4) must be $\approx$0.84.

B. The S isotope shift

The S and Se ISs involve the triply degenerate τ_2 mode, the only one that includes a displacement of the chalcogen atom. Within the preceding assumption, the same mode softening is responsible for an IS when $^{32}S^{28}Si_4$ is replaced by $^{34}S^{28}Si_4$, namely,

$$\delta_S=\frac{3\hbar\omega_1^e}{2}[\sqrt{1+\Lambda_{34}}-\sqrt{1+\Lambda_{32}}]\left(1-\sqrt{\frac{k_g}{k_e}}\right), \tag{5}$$

where the indexes correspond to the masses of the S isotopes. The same causes producing the same effects, with the above value of k_g/k_e, the predicted ^{32}S–^{34}S IS for $1s(T_2)\Gamma_7$ is negative while the experimental value is $+69$ μeV and this confirms that the chalcogen isotope shift must include another mechanism.

One important point has been omitted in the above description of the S IS, namely the electron-τ_2 local mode coupling. If it has no effect on the ground state, which is an orbital singlet, it modifies the excited states, which originate from an orbital triplet, through a $T_2\otimes\tau_2$ vibronic coupling. The electron-local mode coupling constant V_T has a purely electronic origin and the Jahn-Teller energy E_{JT} is therefore independent of the mass of the chalcogen atom. It can be written $E_{JT}=2V_T^2/3\mu\omega_5^2$, where μ is the reduced mass of the

τ_2 mode. The term $\mu\omega_5^2$ is simply the mass-independent spring constant. The energy of the lower vibronic excited state[22] becomes $E_{\rm el}-E_{\rm JT}+\gamma\hbar\omega_5^e$. The two first terms of this expression are independent of the mass of the chalcogen atom and γ is a factor that can take values between $\approx$1.2 and 3/2.[22] When the zero-point energy in the excited state $3\hbar\omega_5^e/2$ is replaced by $\gamma\hbar\omega_5^e$, expression (5) reads

$$\delta_S=\hbar\omega_1^e[\sqrt{1+\Lambda_{34}}-\sqrt{1+\Lambda_{32}}]\left(\gamma-\frac{3}{2}\sqrt{\frac{k_g}{k_e}}\right). \qquad (6)$$

For $\gamma<\frac{3}{2}\sqrt{k_g/k_e}$, the IS δ_S is positive, as observed. With the above value of k_g/k_e, γ must be less than 1.374 in order to get a positive value of the IS. This corresponds[22] to a value of $\sqrt{3E_{\rm JT}/2\hbar\omega_5^e}$ (the k abscissa unit of Fig. 1 of Ref. 22) larger than 0.7 and this means that for a rather moderate strength of the $T_2\otimes\tau_2$ vibronic coupling, the chalcogen IS becomes positive. To reproduce the observed value of δ_S, γ must be 1.327 which corresponds[22] to $E_{\rm JT}/\hbar\omega_5^e\approx0.5$. The value of ω_5 derived from the estimated frequency of ω_1 used above for the SSi_4 cluster yields a value of the Jahn-Teller energy of $\approx$45.6 meV for the $1s(T_2)$ state of S^+. This value of $E_{\rm JT}$ provides an explanation for about 75% of the difference near 60 meV between the experimental energy of the $1s(T_2)$ state of S^+ and the one obtained from effective mass theory (Table I).

As already mentioned in Sec. II, the effect of an uniaxial stress on the $1s(T_2)$ states is smaller than expected from the combination of the effective mass approximation and deformation potential approximations.[16] The $T_2\otimes\tau_2$ vibronic coupling discussed above reduces the effect of nontotally symmetric operators;[22] thus it contributes to the effectively observed reduction of the effect of uniaxial stresses. Using the results of Ref. 22 together with the value of $E_{\rm JT}/\hbar\omega_5^e$ quoted above, one obtains a reduction factor around 0.4, very close to the factor of 0.37 observed experimentally.[16]

It turns out that a negative ^{34}S IS has been reported some years ago for $2p_\pm(S^+)$ in silicon.[23] It was obtained by measuring the energy shift of the $2p_\pm$ peak in a sample enriched with about 90% of ^{34}S. The FWHM of $2p_\pm(S^+)$ measured at 9 K in this experiment was $\sim$0.9 meV and the shift found to be negative for ^{34}S, about two times larger (-0.14 meV) than the one, positive, reported here for $1s(T_2)$. The same result was also found for the other lines (limited in energy to $2p_0$ and above) of this ^{34}S-enriched sample.[23] A possible explanation for this observation could be the absence (or the weakness) of $T_2\otimes\tau_2$ vibronic coupling in the $2p_\pm$ excited state and the fact that the electron is still more delocalized in the $2p_\pm$ state than in the $1s(T_2)$ states. The first point is reinforced by the fact that the effect of stress follows the effective mass theory-deformation potential approximations. Another possibility to explain the above experimental result is the fact that, in this particular experiment, the samples were reported to be illuminated with white light, creating electron-hole pairs so that the S atoms could be partially neutralized. If the compensation ratio was different in the samples doped with natural S and ^{34}S, so was the perturbation of the electrons in the excited states and a negative shift of the lines can be produced by a stronger inhomogeneous Stark effect.

IV. CONCLUSION

We have produced evidence of two opposite ISs of the $1s(T_2)$ components of the spectrum of S^+ in silicon and we have shown that they can explain the profile of one of the corresponding lines of Se^+ in silicon. The negative Si shift can be explained by a softening of the chalcogen–Si bonds in the ground state due to the localization of the donor electron. The positive chalcogen IS can be understood in terms of a vibronic coupling of the excited electronic triplet state with the triply degenerate local vibrational mode involving a displacement of the chalcogen atom. This effect combined with the bond softening is shown to be able to produce a positive S IS. Incidentally, we have shown that this vibronic coupling accounts for most of the energy difference with effective mass theory as well as for the stress effect anomalies observed for the $1s(T_2)$ level of S^+.

ACKNOWLEDGMENT

The ^{33}S-enriched sample was kindly provided by Professor C. A. J. Ammerlaan. We acknowledge stimulating discussions with H. J. von Bardeleben on EPR results on the samples and the help of L. Siozade in the curve fitting procedure.

[1] G. Davies, E. C. Lightowlers, and M. do Carmo, J. Phys. C **16**, 5503 (1983).
[2] K. Pressel, K. Thonke, A. Dörnen, and G. Pensl, Phys. Rev. B **43**, 2239 (1991).
[3] A. Hoffmann and U. Scherz, J. Cryst. Growth **101**, 385 (1990).
[4] W. Kohn and J. M. Luttinger, Phys. Rev. **98**, 915 (1955).
[5] H. G. Grimmeiss, E. Janzén, and K. Larsson, Phys. Rev. B **25**, 2627 (1982).
[6] J. B. Wright and A. Mooradian, Phys. Rev. Lett. **67**, 608 (1967).
[7] K. Jain and M. V. Klein, Phys. Rev. B **13**, 5448 (1976).
[8] W. E. Krag, in *Proceedings of the 10th International Conference on Physics and Semiconductors*, edited by S. P. Keller, J. C. Hensel, and F. Stern (US Atomic Energy Commission, Oak Ridge, Tennessee, 1970), p. 271.
[9] H. G. Grimmeiss and E. Janzén, in *Handbook on Semiconductors*, edited by T. S. Moss, in *Materials, Properties and Preparation*, edited by S. Mahajan (North-Holland, Amsterdam, 1994), Vol. 3b, p. 1755.
[10] G. W. Ludwig, Phys. Rev. **137**, A1520 (1965).
[11] E. E. Haller, B. Joós, and L. M. Falicov, Phys. Rev. B **21**, 4729 (1980).
[12] B. Clerjaud, D. Côte, A. Lebkiri, C. Naud, J. M. Baranowski, K.

Pakula, D. Wasik, and T. Suski, Phys. Rev. B **61**, 8238 (2000).
[13] W. E. Krag, W. H. Kleiner, and H. J. Zeiger, Phys. Rev. B **33**, 8304 (1986).
[14] E. Janzén, R. Stedman, G. Grossmann, and H. G. Grimmeiss, Phys. Rev. B **29**, 1907 (1984).
[15] P. Wagner, in *Properties of Crystalline Silicon*, edited by R. Hull, EMIS Datareviews Series No. 20 (INSPEC, London, 1999), p. 573.
[16] K. Bergman, G. Grossmann, H. G. Grimmeiss, Michael Stavola, and Robert E. McMurray, Jr., Phys. Rev. B **39**, 1104 (1989).
[17] B. Pajot, E. Artacho, C. A. J. Ammerlaan, and J. M. Spaeth, J. Phys.: Condens. Matter **7**, 7077 (1995).
[18] M. D. Sciacca, A. K. J. Mayur, H. Kim, I. Miotkowski, A. K. Ramdas, and S. Rodriguez, Phys. Rev. B **53**, 12878 (1996).
[19] V. Heine and C. H. Henry, Phys. Rev. B **11**, 3795 (1975).
[20] J. E. Rosenthal, Phys. Rev. **45**, 538 (1934).
[21] J. F. Angress, A. R. Goodwin, and S. D. Smith, Proc. R. Soc. London, Ser. A **308**, 111 (1968).
[22] M. Caner and R. Englman, J. Chem. Phys. **44**, 4054 (1966).
[23] R. A. Forman, Appl. Phys. Lett. **37**, 776 (1980).